Self-consistent localized KKR scheme for surfaces and interfaces

L. Szunyogh
Institut für Technische Elektrochemie, Technische Universität Wien, Getreidemarkt 9/158, A-1060 Wien, Austria and Physical Institute, Technical University Budapest, Budafoki út 8, H-1111 Budapest, Hungary

B. Újfalussy
Institut für Technische Elektrochemie, Technische Universität Wien, Getreidemarkt 9/158, A-1060 Wien, Austria and Research Institute for Solid State Physics, Hungarian Academy of Sciences, H-1525 Budapest, P.O. Box 49, Hungary

P. Weinberger
Institut für Technische Elektrochemie, Technische Universität Wien, Getreidemarkt 9/158, A-1060 Wien, Austria

J. Kollár
Research Institute for Solid State Physics, Hungarian Academy of Sciences, H-1525 Budapest, P.O. Box 49, Hungary
(Received 9 July 1993)

A Green's-function technique is presented that describes the electronic properties of surfaces and interfaces in the framework of multiple-scattering theory as based on localized structure constants. Results of self-consistent calculations are presented for the Cu (111), (110), and (100) surfaces. The obtained surface densities of states and work functions are in good agreement with previous calculations.

I. INTRODUCTION

During the past years a great deal of interest has been devoted to the electronic structure of surfaces and interfaces, because of their interesting physical properties, which in turn gave rise to different classes of technologically important systems and devices. Theoretical self-consistent *ab initio* Green's-function methods have been developed both within the linear muffin-tin orbital (LMTO) and the multiple-scattering theories. The LMTO methods have been successfully applied to surfaces of several systems.[1–8] These calculations are based on the so-called tight-binding (TB) LMTO scheme, originally developed by Andersen and Jepsen.[9] The main feature of this approach is the tridiagonal shape of the Hamiltonian due to the use of the short range structure constants. At the same time multiple-scattering related methods have been developed, using the removal invariance principle[10,11] or the layer-doubling technique.[12,13] Calculations based on these methods concentrated mainly on planar defects in metals and alloys.[12–16]

In the present paper we describe a localized Korringa-Kohn-Rostoker (KKR) scheme for the calculation of electronic properties of surfaces and interfaces. It is an attempt to unify the pleasant features found in the TB-LMTO method, namely, the short-range structure constants, with the more exact multiple scattering theory. In principle this approach allows us to treat the electronic properties of surfaces and interfaces within multiple-scattering theory without any further approximations.

II. THE SCREENED KKR EQUATIONS

The scattering path operator $\tau(E)$ in real space multiple-scattering theory is given by (see, e.g., Chap. 6 of Ref. 17 and references therein)

$$\boldsymbol{\tau}(E)=[\boldsymbol{t}(E)^{-1}-\boldsymbol{G}(E)]^{-1} , \tag{1}$$

where in terms of a supermatrix notation

$$\boldsymbol{\tau}(E)=\{\underline{\tau}^{nm}(E)\},\quad \underline{\tau}^{nm}(E)=\{\tau^{nm}_{LL'}(E)\} , \tag{2}$$

$$\boldsymbol{t}(E)=\{\underline{t}^{n}(E)\delta_{nm}\},\quad \underline{t}^{n}(E)=\{t^{n}_{LL'}(E)\} , \tag{3}$$

$$\boldsymbol{G}(E)=\{\underline{G}^{nm}(E)\},\quad \underline{G}^{nm}(E)=\{G^{nm}_{LL'}(E)\} . \tag{4}$$

Here n and m denote lattice sites, $L=(l,m)$ and $L'=(l',m')$ are (nonrelativistic) angular momentum quantum numbers, and E is the energy. The structure constants $G^{nm}_{LL'}(E)$ are defined by the expansion

$$\begin{aligned}
&-i\sqrt{E}\,h^{+}_{L}(E;\mathbf{r}-\mathbf{R}_n)=\sum_{L'} j_{L'}(E;\mathbf{r}-\mathbf{R}_m)G^{mn}_{L'L}(E)\\
&(|\mathbf{r}-\mathbf{R}_n|>|\mathbf{r}-\mathbf{R}_m|) ,\\
&j_L(E;\mathbf{r})=j_l(\sqrt{E}r)Y_L(\hat{\mathbf{r}}) ,\\
&h^{+}_{L}(E;\mathbf{r})=h^{+}_{l}(\sqrt{E}r)Y_L(\hat{\mathbf{r}}) ,
\end{aligned} \tag{5}$$

where $\mathbf{R}_n$ and $\mathbf{R}_m$ are the position vectors of the sites n and m, j_l and h^{+}_{l} spherical Bessel functions and the spherical Hankel functions of first order, respectively, and Y_L denote spherical harmonics. The regular single-site scattering solutions $R^{n}_{L}(E;\mathbf{r})$ belonging to the potential centered at $\mathbf{R}_n$ are normalized at the muffin-tin radius by means of the following linear combination of the functions j_L and h^{+}_{L}:

$$\begin{aligned}
R^{n}_{L}(E;\mathbf{r})=&\,j_L(E;\mathbf{r}-\mathbf{R}_n)\\
&-i\sqrt{E}\sum_{L'} h^{+}_{L'}(E;\mathbf{r}-\mathbf{R}_n)t^{n}_{L'L}(E) ,
\end{aligned} \tag{6}$$

where $t^n_{LL'}(E)$ denotes the single-site scattering ($\mathbf{t}$) matrix appearing in (3). The Green's function is then given by

$$\mathcal{G}(\mathbf{r}+\mathbf{R}_n,\mathbf{r}'+\mathbf{R}_m;E) = \mathrm{Tr}\{\underline{R}^n(E;\mathbf{r})\underline{t}^n(E)^{-1}\underline{\tau}^{nm}(E)\underline{t}^m(E)^{-1}\underline{R}^m(E;\mathbf{r}')^\dagger - \delta_{nm}\underline{J}^n(E;\mathbf{r})\underline{t}^n(E)^{-1}\underline{R}^n(E;\mathbf{r}')^\dagger\} , \quad (7)$$

where Tr denotes the trace of a matrix. In (7) $\underline{R}^n(E;\mathbf{r})$ and $\underline{J}^n(E;\mathbf{r})$ denote diagonal matrices of elements $R^n_L(E;\mathbf{r})$ and $J^n_L(E;\mathbf{r})$, respectively. $J^n_L(E;\mathbf{r})$ are single-site scattering solutions irregular at the origin that join smoothly to $j_L(E;\mathbf{r}-\mathbf{R}_n)$ beyond the muffin-tin radius.

Our aim is now to transform $\boldsymbol{G}(E)$ to have the spacially shortest possible range. For this reason, according to Andersen and Jepsen,[9] let us introduce the functions

$$j^\alpha_L(E;\mathbf{r}) = j_L(E;\mathbf{r}) - i\sqrt{E}\,\hat{\alpha}_l(E)h^+_L(E;\mathbf{r}) , \quad (8)$$

where the functions $\hat{\alpha}_l(E)$ are (energy dependent) screening parameters. The whole idea of screening is based on an expansion analogous to (5) in terms of the functions j^α_L, which in turn implies the following transformation of the structure constants:

$$\boldsymbol{G}^\alpha(E) = \boldsymbol{G}(E)[\boldsymbol{I}-\hat{\boldsymbol{\alpha}}(E)\boldsymbol{G}(E)]^{-1},$$
$$\boldsymbol{G}^\alpha(E) = \boldsymbol{G}(E)+\boldsymbol{G}(E)\hat{\boldsymbol{\alpha}}(E)\boldsymbol{G}^\alpha(E) \quad (9)$$
$$[\hat{\boldsymbol{\alpha}}(E)=\{\underline{\hat{\alpha}}(E)\delta_{nm}\},\ \underline{\hat{\alpha}}(E)=\{\hat{\alpha}_l(E)\delta_{LL'}\}] ,$$

where $\boldsymbol{G}^\alpha(E)$ is referred to as a screened representation of $\boldsymbol{G}(E)$. The details of the derivation of this transformation can be found in Ref. 18. In Appendix A the method is discussed that we used to find the parameters $\hat{\alpha}_l(E)$ defining the most localized representation $\boldsymbol{G}^\alpha(E)$.

By reexpressing (6) with respect to the functions j^α_L, one gets

$$R^n_L(E;\mathbf{r}) = j^\alpha_{L'}(E;\mathbf{r}-\mathbf{R}_n) - i\sqrt{E}\sum_{L'} h^+_{L'}(E;\mathbf{r}-\mathbf{R}_n)t^{\alpha;n}_{L'L}(E) , \quad (10)$$

defining the corresponding single-site scattering matrices in the new representation as

$$t^\alpha(E) = t(E)-\hat{\boldsymbol{\alpha}}(E) , \quad (11)$$

and, consequently, similarly to (3) the supermatrix of $t^\alpha(E)$. In analogy to (1), the scattering path operator can now be defined in the screened representation as

$$\tau^\alpha(E) = [t^\alpha(E)^{-1}-\boldsymbol{G}^\alpha(E)]^{-1} . \quad (12)$$

By using (1), (9), (11), and (12) a site-diagonal transformation between $\tau(E)$ and $\tau^\alpha(E)$ can be established, namely,

$$\underline{\tau}^{nm}(E) = \underline{t}^n(E)\underline{t}^{\alpha,n}(E)^{-1}\underline{\tau}^{\alpha,nm}(E)\underline{t}^{\alpha,m}(E)^{-1}\underline{t}^m(E) - \delta_{nm}\underline{t}^n(E)\underline{t}^{\alpha,n}(E)^{-1}\underline{\hat{\alpha}}(E) . \quad (13)$$

It is straightforward to show from (8) and (13) that the Green's function is invariant with respect to the screening transformation, i.e.,

$$\mathcal{G}(\mathbf{r}+\mathbf{R}_n,\mathbf{r}'+\mathbf{R}_m;E) = \mathrm{Tr}\{\underline{R}^n(E;\mathbf{r})\underline{t}^{\alpha,n}(E)^{-1}\underline{\tau}^{\alpha,nm}(E)\underline{t}^{\alpha,m}(E)^{-1}\underline{R}^m(E;\mathbf{r}')^\dagger - \delta_{nm}\underline{J}^{\alpha,n}(E;\mathbf{r})\underline{t}^{\alpha,n}(E)^{-1}\underline{R}^n(E;\mathbf{r}')^\dagger\} . \quad (14)$$

It should be noted that now the irregular solutions $J^{\alpha,n}_L(E;\mathbf{r})$ match $j^\alpha_L(E;\mathbf{r}-\mathbf{R}_n)$ at the muffin-tin radius, while according to (10) the regular scattering solutions $R^n_L(E;\mathbf{r})$ remain representation invariant.

III. APPLICATION TO SYSTEMS WITH TWO-DIMENSIONAL TRANSLATIONAL INVARIANCE

The advantage of a screened representation becomes obvious when applied to surfaces and interfaces of crystals, i.e., to two-dimensional translation invariant systems. In the following, vectors parallel or perpendicular to the plane of the surface (interface) are labeled by subscripts $\|$ or $\perp$, respectively. Each atomic position vector $\mathbf{R}_n$ can then be expressed in terms of a vector $\mathbf{C}_p$ and a two-dimensional lattice vector $\mathbf{R}_\|$:

$$\mathbf{R}_n = \mathbf{C}_p+\mathbf{R}_\| , \quad (15)$$

where, by neglecting lattice relaxation effects, $\mathbf{C}_p$ is a multiple of a generating vector $\mathbf{C}_0$ which connects two neighboring atomic layers. In this case, the two-dimensional lattice Fourier transform of the screened structure constants, which is generally defined by

$$\underline{G}^{\alpha,pq}(\mathbf{k}_\|;E) = \sum_{\mathbf{R}_\|} e^{i\mathbf{k}_\|\cdot\mathbf{R}_\|}\underline{G}^\alpha(\mathbf{C}_p+\mathbf{R}_\|,\mathbf{C}_q;E) , \quad (16)$$

can be calculated as[6]

$$\underline{G}^{\alpha,pq}(\mathbf{k}_\|;E) = \frac{d}{2\pi}e^{-i\mathbf{k}_\|\cdot(\mathbf{C}_{p,\|}-\mathbf{C}_{q,\|})}\int_{-\pi/d}^{\pi/d} dk_\perp e^{-ik_\perp\cdot(\mathbf{C}_{p,\perp}-\mathbf{C}_{q,\perp})}\underline{G}^\alpha(\mathbf{k}_\|+\mathbf{k}_\perp\hat{\mathbf{z}};E) , \quad (17)$$

where d denotes the layer spacing. Here we made use of the fact that scaling transformation (9) applies to all projections of the screened structure constants,

$$\underline{G}^\alpha(\mathbf{k};E) = \underline{G}(\mathbf{k};E)[\underline{I}-\underline{\hat{\alpha}}(E)\underline{G}(\mathbf{k};E)]^{-1} , \quad (18)$$

where $\underline{G}(\mathbf{k},E)$ is the "usual" three-dimensional lattice Fourier transform of the unscreened structure constants.

The short range behavior of the screened structure constants suggests that the following assumption can be made:

$$\underline{G}^{\alpha,pq}(\mathbf{k}_\|;E) = \underline{0} \quad \text{if } |p-q|>N , \quad (19)$$

where N is a suitably chosen parameter. Now it is natural to introduce the concept of principal layers.[19] A principal

layer includes N subsequent physical (or "atomic") layers and will be denoted by capital letters, e.g., P and Q. The supermatrix of the structure constants can then be partitioned with respect to principal layers

$$\boldsymbol{G}^{\alpha}(\mathbf{k}_{\parallel};E)=\{\underline{\underline{G}}^{\alpha,PQ}(\mathbf{k}_{\parallel};E)\} , \tag{20}$$

where

$$\underline{\underline{G}}^{\alpha,PQ}(\mathbf{k}_{\parallel};E)=\{\underline{G}^{\alpha,pq}(\mathbf{k}_{\parallel};E)\},\quad p=(P-1)N,(P-1)N+1,\ldots,PN-1\quad q=(Q-1)N,(Q-1)N+1,\ldots,QN-1 . \tag{21}$$

Obviously, a principal layers couples to the next principal layer only, i.e., the supermatrix of structure constants (20) is tridiagonal with respect to principal layer indices

$$\underline{\underline{G}}^{\alpha,PQ}(\mathbf{k}_{\parallel};E)=\underline{\underline{G}}^{\alpha,00}(\mathbf{k}_{\parallel};E)\delta_{PQ}+\underline{\underline{G}}^{\alpha,01}(\mathbf{k}_{\parallel};E)\delta_{P,Q-1}+\underline{\underline{G}}^{\alpha,10}(\mathbf{k}_{\parallel};E)\delta_{P,Q+1} . \tag{22}$$

The two-dimensional lattice Fourier transform of the scattering path operator in the screened representation is therefore given by

$$\boldsymbol{\tau}^{\alpha}(\mathbf{k}_{\parallel};E)=[\boldsymbol{t}^{\alpha}(E)^{-1}-\boldsymbol{G}^{\alpha}(\mathbf{k}_{\parallel};E)]^{-1} , \tag{23}$$

where

$$\boldsymbol{t}^{\alpha}(E)=\{\underline{t}^{\alpha,P}(E)\delta_{PQ}\},\quad \underline{t}^{\alpha,P}(E)=\{\underline{t}^{\alpha,p}(E)\delta_{pq}\} ,$$

$$\boldsymbol{\tau}^{\alpha}(\mathbf{k}_{\parallel};E)=\{\underline{\tau}^{\alpha,PQ}(\mathbf{k}_{\parallel};E)\},\quad \underline{\tau}^{\alpha,PQ}(E)=\{\underline{\tau}^{\alpha,pq}(E)\} .$$

In the following, the inverse of this scattering path operator is denoted by $\boldsymbol{M}$,

$$\boldsymbol{M}=\boldsymbol{\tau}^{\alpha}(\mathbf{k}_{\parallel};E)^{-1} . \tag{24}$$

For a surface or an interface the parent lattice consists of three regions, where physical properties differ from each other, namely, a *left semi-infinite system* (L), a *right semi-infinite system* (R), *and an intermediate interface region* (I). These regions are defined by the following numbering scheme for principal layers:

$$\begin{aligned} &L:\ -\infty<P\le 0 ,\\ &I:\ 1\le P\le n ,\\ &R:\ n+1\le P<\infty . \end{aligned} \tag{25}$$

This formal partitioning of the parent infinite system implies that one can also partition the matrix $\boldsymbol{M}$ as follows:

$$\boldsymbol{M}=\begin{pmatrix} \boldsymbol{M}_{L,L} & \boldsymbol{M}_{L,I} & 0 \\ \boldsymbol{M}_{I,L} & \boldsymbol{M}_{I,I} & \boldsymbol{M}_{I,R} \\ 0 & \boldsymbol{M}_{R,I} & \boldsymbol{M}_{R,R} \end{pmatrix} . \tag{26}$$

The explicit forms of the blocks of $\boldsymbol{M}$ are listed in Appendix B. Of course, the number of layers included in the interface region is somewhat arbitrary. In practical calculations it has to be checked therefore whether convergency is achieved in terms of the number of physical layers in the interface region.

We are left now with the task to invert an infinite block-tridiagonal matrix. It should be recalled that this block-tridiagonal shape is a direct consequence of the short range structure constants. In order to calculate the quantity $\tau^{\alpha}_{I,I}(\mathbf{k}_{\parallel};E)$, namely, the interface-interface block of the scattering path operator of the whole system, the following inversion has to be performed:

$$\begin{aligned} \tau^{\alpha}_{I,I}(\mathbf{k}_{\parallel};E)=[&\boldsymbol{M}_{I,I}-\boldsymbol{M}_{I,L}(\boldsymbol{M}_{L,L})^{-1}\boldsymbol{M}_{L,I}\\ &-\boldsymbol{M}_{I,R}(\boldsymbol{M}_{R,R})^{-1}\boldsymbol{M}_{R,I}]^{-1} . \end{aligned} \tag{27}$$

Focusing for a moment only on those terms in the above equation which contain products of infinite matrices and by taking into account the explicit forms of the blocks involved (see Appendix B), it is easy to see that only the blocks

$$\underline{\underline{\Delta}}_L=[(\boldsymbol{M}_{L,L})^{-1}]^{00},\quad \underline{\underline{\Delta}}_R=[(\boldsymbol{M}_{R,R})^{-1}]^{n+1,n+1} \tag{28}$$

contribute to these products, namely,

$$[\boldsymbol{M}_{I,L}(\boldsymbol{M}_{L,L})^{-1}\boldsymbol{M}_{L,I}]^{PQ}=\underline{\underline{M}}^{10}\underline{\underline{\Delta}}_L\underline{\underline{M}}^{01}\delta_{P,1}\delta_{Q,1} , \tag{29}$$

$$[\boldsymbol{M}_{I,R}(\boldsymbol{M}_{R,R})^{-1}\boldsymbol{M}_{R,I}]^{PQ}=\underline{\underline{M}}^{01}\underline{\underline{\Delta}}_R\underline{\underline{M}}^{10}\delta_{P,n}\delta_{Q,n} . \tag{30}$$

The quantities $\underline{\underline{\Delta}}_L$ and $\underline{\underline{\Delta}}_R$ are related to the surface Green's function in a tight-binding formalism.[1,2,6,19] They are in fact the surface scattering path operators corresponding to the lower right and upper left diagonal blocks of the respective semi-infinite matrix. These scattering path operators can be calculated as described in Ref. 2, namely, from the conditions

$$\underline{\underline{\Delta}}_L=(\underline{\underline{M}}^{L}-\underline{\underline{M}}^{10}\underline{\underline{\Delta}}_L\underline{\underline{M}}^{01})^{-1} , \tag{31}$$

$$\underline{\underline{\Delta}}_R=(\underline{\underline{M}}^{R}-\underline{\underline{M}}^{01}\underline{\underline{\Delta}}_R\underline{\underline{M}}^{10})^{-1} . \tag{32}$$

In terms of these two quantities, the scattering path operator in the interface region is then given by

$$\begin{aligned} [\tau^{\alpha}_{I,I}(\mathbf{k}_{\parallel};E)^{-1}]^{PQ}=&[\underline{t}^{\alpha,P}(E)^{-1}-\underline{\underline{G}}^{\alpha,00}(\mathbf{k}_{\parallel};E)]\delta_{PQ}-\underline{\underline{G}}^{\alpha,01}(\mathbf{k}_{\parallel};E)\delta_{P,Q-1}-\underline{\underline{G}}^{\alpha,10}(\mathbf{k}_{\parallel};E)\delta_{P,Q+1}\\ &-\underline{\underline{G}}^{\alpha,10}(\mathbf{k}_{\parallel};E)\underline{\underline{\Delta}}^{\alpha}_L(\mathbf{k}_{\parallel};E)\underline{\underline{G}}^{\alpha,01}(\mathbf{k}_{\parallel};E)\delta_{P,1}\delta_{Q,1}-\underline{\underline{G}}^{\alpha,01}(\mathbf{k}_{\parallel};E)\underline{\underline{\Delta}}^{\alpha}_R(\mathbf{k}_{\parallel};E)\underline{\underline{G}}^{\alpha,10}(\mathbf{k}_{\parallel};E)\delta_{P,n}\delta_{Q,n} . \end{aligned} \tag{33}$$

All the scattering paths in the infinite system which start and end in the interface region are now properly taken into account. Finally, the site representation of the screened scattering path operator can be obtained in the interface region by the following Brillouin zone integral:

$$\underline{\tau}^{\alpha,nm}(E)=\frac{1}{\Omega}\int d\mathbf{k}_{\parallel}e^{-i\mathbf{k}_{\parallel}\cdot(\mathbf{R}_{\parallel}-\mathbf{R}'_{\parallel})}\underline{\tau}^{\alpha,pq}(\mathbf{k}_{\parallel};E)\ ,$$
$$\mathbf{R}_n=\mathbf{C}_p+\mathbf{R}_{\parallel},\quad \mathbf{R}_m=\mathbf{C}_q+\mathbf{R}'_{\parallel}\ , \tag{34}$$

where Ω is the volume of the two-dimensional Brillouin zone.

Layer dependent physical quantities such as densities of states, charge densities, or the moments of charge densities can easily be calculated using (7) and (13):

$$n_p(E)=-\frac{2}{\pi}\mathrm{Im}\int d\mathbf{r}\,\mathcal{G}(\mathbf{r}+\mathbf{C}_p,\mathbf{r}+\mathbf{C}_p;E)\ , \tag{35}$$

$$\rho_p(\mathbf{r})=-\frac{2}{\pi}\mathrm{Im}\int_{\mathcal{C}}dz\,\mathcal{G}(\mathbf{r}+\mathbf{C}_p,\mathbf{r}+\mathbf{C}_p;z)\ , \tag{36}$$

$$Q_p^L=\frac{\sqrt{4\pi}}{2l+1}\int d\mathbf{r}\,r^l\rho_p(\mathbf{r})Y_L(\hat{\mathbf{r}})\ . \tag{37}$$

In (36) $\mathcal{C}$ denotes an integration contour in the upper half of the complex energy plane, which starts at a real energy point well below the valence band and ends at the Fermi energy.[12]

In order to obtain charge self-consistency, the new layer dependent muffin-tin potentials consisting of the electrostatic and of the exchange-correlation potential are of the following form (see, e.g., Chap. 10 in Ref. 17):

$$V_p(r)=-\frac{2Z_p}{r}+\frac{8\pi}{r}\int_0^r dr'\,r'^2\rho_p(r')+8\pi\int_r^{S_p}dr'\,r'\rho_p(r')$$
$$+V_p^{\mathrm{Mad}}-4\pi\bar{\rho}_pS_p^2-V^{EC}+V^{\mathrm{xc}}[\rho_p(r)]-V^{\mathrm{xc}}[\bar{\rho}_0]\ , \tag{38}$$

where Z_p and S_p refer to the atomic number and the muffin-tin radius associated with sites in the layer p, respectively. In particular for surface calculations, because of the asymmetry of the system, it is necessary to introduce an inhomogeneous interstitial charge density distribution $\bar{\rho}_p$, varying from layer to layer, whereas $\bar{\rho}_0$ denotes the interstitial charge density for the bulk. The solution of Poisson's equation for a system inhomogeneous with respect to one direction is given in Appendix C, together with explicit formulas of the Madelung potentials V_p^{Mad} for surfaces. It is worthwhile to note that the bulk interstitial level of the electrostatic potential V^{EC} and that of the exchange-correlation potential $V^{\mathrm{xc}}[\bar{\rho}_0]$ have to be considered as constant shifts to the potential throughout all space. In Appendix C the constant vacuum potential level V_{vac} is also given, from which the work function can be calculated as follows:

$$W=V_{\mathrm{vac}}-E_F\ , \tag{39}$$

where E_F is the Fermi level.

IV. APPLICATION TO THE SURFACE OF COPPER METAL

For the purpose of test calculations we chose the three principal surfaces of fcc copper. The latter parameter was 6.831 a.u., with a corresponding muffin-tin radius of 2.451 a.u. The core states were treated within the frozen core approximation. In all calculations we used the Gunnarsson-Lundquist exchange-correlation potential and the energy integration was performed by means of Gaussian quadrature with 12 points on a semicircle. The two-dimensional Brillouin zone integral (34) was evaluated according to Ref. 20. To ensure rather fast convergency during the self-consistent iterations we mixed potentials by using a combination of simple mixing and a three-iteration Anderson mixing.[21,22]

First, we carried out a self-consistent bulk calculation for fcc copper. The technique described in Sec. III applies trivially also for bulk calculations by implying that all layer dependent quantities are the same in each layer. Since, in principal, a bulk calculation should not depend on the choice of the surface direction, it had to be examined carefully whether convergency can be obtained to satisfy this requirement in terms of the cutoff parameter N, see (19), and in terms of the number of special k points in the irreducible segment of the corresponding two-dimensional (2D) Brillouin zone (BZ). The Fermi energy was converged in each case to be stable up to 10^{-7} Ry. We found that $N=5$ ensures a relative accuracy of 10^{-4} for E_F. By increasing the number of k points up to 45 for the (100) and (111) directions and up to 49 for the (110) direction we found a relative convergency of 5×10^{-4} for E_F. With these parameters for the BZ integration, the calculated Fermi energies for the three different directions differed from each other well below 1 mRy and amounted to $E_F=0.619$ Ry relative to the muffin-tin zero potential level.

When performing surface calculations we used two principal layers, i.e., ten physical layers for the "interface" region. The ideal vacuum layers were represented by empty spheres characterized by the constant potential V_{vac} as determined by (C20). In order to mimic the decay of the charge density and the $1/r_{\perp}$-like image potential in the vacuum, we included some empty sphere layers into the interface region too. At this point we found an inherent difficulty in describing the vacuum in a muffin-tin geometry. Multiple-scattering theory as mentioned in connection to (38) does not permit to have layer dependent constant potential levels in the interstitial region. Describing, therefore, the flat positive empty sphere potentials in terms of muffin-tin potentials leads to an unphysical picture. Clearly, in order to avoid this discrepancy one should consider space-filling "empty cell" potentials in this region. In the present calculations we approximated these empty cell potentials by spherical potentials extended to the Wigner-Seitz radius, i.e., by using the well known atomic sphere approximation (ASA).

Starting from the bulk potentials for the copper layers, we generally needed about 100 iteration steps to obtain highly converged layer resolved potentials. Since the 2D structure constants had to be calculated only once, one

iteration for 12 energy points and 45 k points took typically 7 min on an IBM RS6000/550 computer. The layer resolved charges and also the vacuum potential level were converged to a relative error of 10^{-5}. According to the required charge neutrality for the system (see Appendix C), the net charge in the interface region was reduced to about 10^{-4} electrons during the self-consistent iterations. The densities of states (DOS's) were then calculated along a line parallel to the real axis, for 100 energy points with an imaginary part of 5 mRy. The calculated bulk and surface DOS's are presented in Fig. 1. In agreement with other calculations[5] the Cu layers below the third layer with respect to the surface are in fact bulklike. In particular for the (111) and (100) surfaces, the Cu atom in the top layer lost some charge, which accumulated mainly in the first empty sphere layer, while in empty sphere layers further apart only a very small fraction of this charge was found. For the more open (110) surface, however, also the Cu layer below the top Cu layer and the second empty sphere layer were involved in charge transfer effects. Irrespective of the surface direction the inclusion of more than two vacuum layers into the interface region had negligible effects on the calculated local DOS's.

As mentioned before, the interfacial empty sphere layers serve to mimic the image potential in the vacuum. Therefore, the calculated work functions are expected to be more sensitive than the local DOS to the number of these layers. This is demonstrated in Table I, where the results corresponding to two, three, and four interfacial vacuum layers are presented for each other. In this table, the row labeled MT refers to the potential model described previously, namely, muffin-tin Cu potentials and ASA empty sphere potentials. In order to compare our results with those obtained by using TB-LMTO ASA, we also performed a set of calculations where not only the vacuum empty cell potentials but also the copper potentials were treated within the ASA. Quite obviously, in this case the contribution to the Madelung potential depending on the interstitial charge densities (C19) vanishes and therefore possible errors due to the somewhat arbitrarily chosen steplike layer dependent interstitial charge densities are excluded from the calculation of the work function. (See also the discussion in the most recent paper by Crampin.[23]) The corresponding results are listed in Table I, namely, in the row labeled ASA, together with the results of TB-LMTO ASA calculations of Ref. 8. Keeping in mind the difference between our ASA calculations and that of Ref. 8, the agreement is excellent.

TABLE I. Calculated work functions (eV) for various Cu surfaces and their convergency with respect to the number of vacuum layers in the interface region. The labels MT and ASA refer to the cases when the Cu potentials were treated within the muffin-tin scheme or within the ASA, respectively. For comparison in the last row we recall the corresponding LMTO-ASA results.

Surface	No. of vacuum layers	MT	ASA	LMTO-ASA[a]
111	2	5.55	5.43	5.30
	3	5.56	5.44	
	4	5.56	5.44	
110	2	3.56	4.53	4.48
	3	4.10	4.98	
	4	4.20	5.04	
100	2	4.98	5.26	5.26
	3	5.03	5.31	
	4	5.03	5.31	

[a]Reference 8.

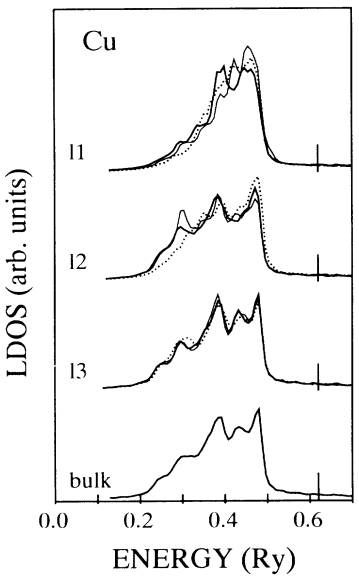

FIG. 1. Calculated layer resolved local densities of states for the (111) (thick solid line), (100) (thin solid line), and (110) (dotted line) surfaces of copper. The top three copper layers are labeled by 11, 12, and 13, respectively. The vertical lines denote the Fermi level.

V. SUMMARY

In summary we can conclude, that the localized KKR scheme presented in this paper is able to calculate the electronic properties of surfaces and interfaces quite accurately. It should be noted, however, that the strict muffin-tin potential model has some shortcomings—in particular for surfaces—which can be resolved in a space-filling full potential scattering formalism. Here the necessary development is forthcoming.

Quite clearly, the main advantage of the present method is its flexibility with respect to an extension to relativistic,[17] relativistic spin-polarized,[24] and anisotropical potential scattering, which formally implies "only" a redefinition of the single-site $\mathbf{t}$ matrix in (6) and of course solving a different Poisson equation (see, e.g., Ref. 25). In particular, the last two applications will provide new aspects in dealing with semi-infinite systems, since in many cases, such as, for example, magnetic interlayer coupling or magnetic coating, it is absolutely necessary to have a clear description for the orientation of the internal magnetic field.

ACKNOWLEDGMENTS

The authors are grateful for many stimulating discussions with J. Kudrnovský, V. Drchal, B. L. Györffy, and C. Sommers. This paper was supported by the Austrian Ministry of Science (Grants Nos. GZ 45.123/4-II/A/4/90 and GZ 49.731/2-24/91) and partially also by the Hungarian National Scientific Research Foundation (Grants Nos. OTKA 2950 and OTKA T7283).

APPENDIX A: DETERMINATION OF THE MOST LOCALIZED REPRESENTATION OF THE STRUCTURE CONSTANTS

In this appendix we solve Eq. (9) in a particular way and show how the most localized representation can be found. In order to obtain the screening functions corresponding to this representation independently of the lattice constant, let us decouple a trivial factor from $\boldsymbol{G}(E)$:

$$\begin{aligned}&\boldsymbol{G}(E)=\boldsymbol{s}(E)^{-1}\boldsymbol{S}(E)\boldsymbol{s}(E)^{-1}\ ,\\ &s^{ij}_{LL'}(E)=\frac{\sqrt{2w}\,(Ew^2)^{l/2}}{(2l-1)!!}\delta_{LL'}\delta_{ij}\ ,\end{aligned}\tag{A1}$$

where w is the some scale of length, e.g., the average Wigner-Seitz radius. It should be noted that $\boldsymbol{S}(E)$ is related to the energy dependent LMTO structure constant matrix in Ref. 18. Now (9) can be rewritten in the form

$$\boldsymbol{S}^{\alpha}(E)=\boldsymbol{S}(E)+\boldsymbol{S}(E)\boldsymbol{\alpha}(E)\boldsymbol{S}^{\alpha}(E)\ ,\tag{A2}$$

which is often referred to as the Dyson equation of screening. $\hat{\boldsymbol{\alpha}}(E)$ in (9) is connected to $\boldsymbol{\alpha}(E)$ by the relation

$$\hat{\alpha}_l(E)=\frac{2w\,(Ew^2)^l\alpha_l(E)}{[(2l-1)!!]^2}\ .\tag{A3}$$

Note that in terms of $\epsilon=Ew^2$, Eq. (A2) and especially $\boldsymbol{\alpha}(E)$ is independent of the scale of length w. The problem now arises when we wish to find the screening function $\boldsymbol{\alpha}(E)$ that produces the structure constants with the shortest possible spacial range. We not only need an effective method to solve the Dyson equation, but also a measure of the localization. Such a theory can be established within the so-called two-center approximation. It is based on the fact that the conventional structure constants in real space can be decoupled into a purely angular and a radial dependent part:[26]

$$S_{L'L}(\mathbf{R};E)=\sum_{\mu=0}^{\min(l',l)}Z^{m'm}_{l'l,\mu}(\hat{\mathbf{R}})I_{l'l,\mu}(R;E)\ ,\tag{A4}$$

where

$$I_{l'l,\mu}(R,E)=\frac{-2i\epsilon^{(l+l'+1)/2}}{(2l'-1)!!(2l-1)!!}\sqrt{(2l+1)(2l'+1)}(-1)^{\mu}\sum_{l''}(2l''+1)i^{l'-l-l''}\begin{pmatrix}l' & l & l''\\ -\mu & \mu & 0\end{pmatrix}\begin{pmatrix}l' & l & l''\\ 0 & 0 & 0\end{pmatrix}h^{+}_{l''}(\sqrt{\epsilon}R/w)\tag{A5}$$

and

$$Z^{m'm}_{l'l,\mu}(\hat{\mathbf{R}})=(2-\delta_{\mu 0})(-1)^{m'-\mu}\sum_{\lambda}\sqrt{4\pi(2\lambda-1)}\begin{pmatrix}l' & l & \lambda\\ -\mu & \mu & 0\end{pmatrix}\begin{pmatrix}l' & l & \lambda\\ -m' & m & m'-m\end{pmatrix}Y^{*}_{\lambda,m'-m}(\hat{\mathbf{R}})\ .\tag{A6}$$

By supposing the same form for the screened structure constants

$$S^{\alpha}_{L'L}(\mathbf{R};E)=\sum_{\mu=0}^{\min(l',l)}Z^{m'm}_{l'l,\mu}(\hat{\mathbf{R}})I^{\alpha}_{l'l,\mu}(R;E)\ ,\tag{A7}$$

it has been shown by Kollár and Újfalussy[27] that the Dyson equation can be written in terms of the exact (A4) and the approximate (A7) two-center integrals:

$$I^{\alpha}_{\Lambda}(n,E)=I_{\Lambda}(n,E)+\sum_{n'\neq 0}\sum_{\Lambda'}Z_{\Lambda,\Lambda'}(n,n')I^{\alpha}_{\Lambda'}(n',E)\ ,\tag{A8}$$

where we introduced a unified subscript $\Lambda=(LL',\mu)$, and n,n' denote the different atomic shells.[27] Note that (A8) is a matrix equation in atomic shells only, and because of that, it is much smaller in size. For any (fixed) energy, it is also possible to define a function Γ based on Eq. (A8) which has a minimum, if the most localized representation is found:

$$\Gamma_{n_0}(\{\alpha\})=\sum_{n=n_0}^{\infty}\sum_{\Lambda}|I^{\alpha}_{\Lambda}(n)|^2\ .\tag{A9}$$

Clearly, the minimum of Γ_{n_0} has to be found for every energy point of interest. Pairs of $\{\alpha_l\},E$ define then the representation where the structure constants have the shortest possible spacial range.

It yet has to be shown that the two-center approximation (A7) is good enough for the search of the minimum of Γ. This can be easily accomplished by comparing the matrices $\boldsymbol{S}^{\alpha}$ calculated by (A7) and (A8) (using the two-center approximation), with the exact solution of the Dyson equation. By solving Eq. (A2) in k space, as in (18), and by a Brillouin zone integration, the exact $\boldsymbol{S}^{\alpha}$ matrices in the site representation can be calculated. By comparing these two cases, one can see that the screening functions obtained in the two-center approximation indeed localized the structure constants. The effect of screening is illustrated in Fig. 2 where the screened and unscreened two-center integrals are shown. It is neces-

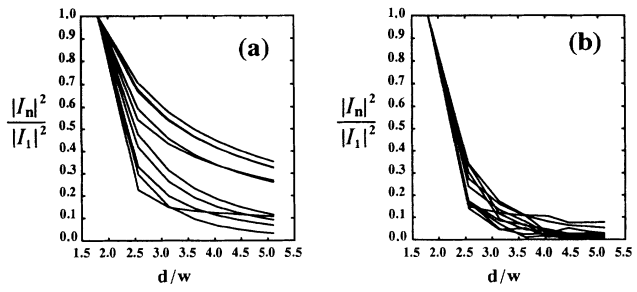

FIG. 2. Relative change of the (a) unscreened and (b) screened two-center integrals I_n [see Eqs. (A5) and (A8)] for $l \leq 2$ in a fcc lattice with respect to the radius of atomic shells d, scaled to the Wigner-Seitz radius w, at $Ew^2=2$.

sary to mention that in the present energy dependent case the screening is not as good as it is in the TB-LMTO method. Therefore the range of the structure constants cannot be restricted to first nearest neighbors only.

APPENDIX B: BLOCKS OF MATRIX M

The explicit expressions of the blocks of the matrix $\boldsymbol{M}$ (26) with respect to the principal layer indices [see also (25)] are given as

$$
\begin{aligned}
(\boldsymbol{M}_{L,L})^{PQ} &= \underline{\underline{M}}^{L}\delta_{PQ}+\underline{\underline{M}}^{01}\delta_{P,Q-1}+\underline{\underline{M}}^{10}\delta_{P,Q+1}\ , \\
(\boldsymbol{M}_{I,I})^{PQ} &= \underline{\underline{M}}^{P}\delta_{PQ}+\underline{\underline{M}}^{01}\delta_{P,Q-1}+\underline{\underline{M}}^{10}\delta_{P,Q+1}\ , \\
(\boldsymbol{M}_{R,R})^{PQ} &= \underline{\underline{M}}^{R}\delta_{PQ}+\underline{\underline{M}}^{01}\delta_{P,Q-1}+\underline{\underline{M}}^{10}\delta_{P,Q+1}\ , \\
(\boldsymbol{M}_{L,I})^{PQ} &= \underline{\underline{M}}^{01}\delta_{P,0}\delta_{Q,1}\ , \\
(\boldsymbol{M}_{I,R})^{PQ} &= \underline{\underline{M}}^{01}\delta_{P,n}\delta_{Q,n+1}\ , \\
(\boldsymbol{M}_{I,L})^{PQ} &= \underline{\underline{M}}^{10}\delta_{P,1}\delta_{Q,0}\ , \\
(\boldsymbol{M}_{R,I})^{PQ} &= \underline{\underline{M}}^{10}\delta_{P,n+1}\delta_{Q,n}\ ,
\end{aligned}
\tag{B1}
$$

where

$$
\begin{aligned}
\underline{\underline{M}}^{L} &= \underline{t}^{\alpha,L}(E)^{-1}-\underline{G}^{\alpha,00}(\mathbf{k}_{\parallel};E)\ , \\
\underline{\underline{M}}^{P} &= \underline{t}^{\alpha,P}(E)^{-1}-\underline{G}^{\alpha,00}(\mathbf{k}_{\parallel};E)\quad (1\leq P\leq n)\ , \\
\underline{\underline{M}}^{R} &= \underline{t}^{\alpha,R}(E)^{-1}-\underline{G}^{\alpha,00}(\mathbf{k}_{\parallel};E)\ , \\
\underline{\underline{M}}^{01} &= -\underline{G}^{\alpha,01}(\mathbf{k}_{\parallel};E)\ , \\
\underline{\underline{M}}^{10} &= -\underline{G}^{\alpha,10}(\mathbf{k}_{\parallel};E)\ .
\end{aligned}
\tag{B2}
$$

APPENDIX C: SOLUTION OF POISSON'S EQUATION FOR LAYERED SYSTEMS

The solution of Poisson's equation for a layered arrangement of point charges embedded into a jellium of constant charge density has been presented by MacLaren *et al.*[12] Quite clearly, their theory works for planar defects in bulk materials, but for surfaces or interfaces of different materials the restriction to a constant interstitial charge density seems to be unphysical. This problem is excluded within the atomic sphere approximation as used for surfaces in the context of the LMTO method[5,6] and very recently also within the layer KKR technique.[23,28] In addition, the dipole term to the electrostatic potential has been also included in these calculations, which is in particular important for a calculation of realistic work functions.[5-8,23,28] In this appendix, by imposing the boundary conditions properly, we present an approximate solution to the 2D Ewald problem for the case when the interstitial charge density varies steplike from layer to layer. In the case of surfaces explicit expressions for the monopole and dipole Madelung constants as well as for the vacuum potential level are given.

In general for the case of a complex 2D system, generated by the nonprimitive 2D translational vectors $\mathbf{a}_\gamma$, the 3D inequivalent lattice positions are given by $\mathbf{r}_{p\gamma}=\mathbf{C}_p+\mathbf{a}_\gamma$, where the $\mathbf{C}_p$ refers to the interlayer vectors in (15). When solving Poisson's equation for point charges embedded into jellium, Ewald's technique has to be used (for the 3D case see Refs. 29 and 30) resulting in the following Ewald potential:

$$
\begin{aligned}
V^{E}(\mathbf{r}) = \sum_{p,\gamma} \bar{q}_{p\gamma}[(1-\delta_{r_\perp,r_{p\gamma,\perp}})\varphi(\mathbf{r}_\parallel-\mathbf{r}_{p\gamma,\parallel};r_\perp-r_{p\gamma,\perp}) \\
+\delta_{r_\perp,r_{p\gamma,\perp}}\varphi_0(\mathbf{r}_\parallel-\mathbf{r}_{p\gamma,\parallel})]+V_\perp(r_\perp)\ .
\end{aligned}
\tag{C1}
$$

Here $\bar{q}_{p\gamma}$ are effective charges, which are defined within a muffin-tin geometry as

$$
\bar{q}_{p\gamma}=Q^{00}_{p\gamma}-Z_{p\gamma}-\frac{4\pi}{3}\bar{\rho}_p S^3_{p\gamma}\ ,
\tag{C2}
$$

where $Q^{00}_{p\gamma}$ is the number of electrons within a sphere labeled by p and γ, $Z_{p\gamma}$ is the corresponding atomic number, $\bar{\rho}_p$ denotes the interstitial charge density in layer p, and $S_{p\gamma}$ is the radius of the sphere. In (C1) the functions describing the 2D electrostatic monopole field are given by[5]

$$
\varphi(\mathbf{r}_\parallel;r_\perp)=\frac{4\pi}{\Omega}\sum_{\mathbf{G}_\parallel\neq 0}\frac{\exp(-|r_\perp\|\mathbf{G}_\parallel|)}{|\mathbf{G}_\parallel|}\cos(|\mathbf{r}_\parallel\mathbf{G}_\parallel|)\ ,
\tag{C3}
$$

$$
\begin{aligned}
\varphi_0(\mathbf{r}_\parallel) = \sum_{\mathbf{R}_\parallel}\frac{2}{|\mathbf{r}_\parallel-\mathbf{R}_\parallel|}\operatorname{erfc}\left[\frac{|\mathbf{r}_\parallel-\mathbf{R}_\parallel|}{2\sigma}\right] \\
-\frac{8\sigma\sqrt{\pi}}{\Omega}+\frac{4\pi}{\Omega}\sum_{\mathbf{G}_\parallel\neq 0}\frac{\operatorname{erfc}(\sigma|\mathbf{G}_\parallel|)}{|\mathbf{G}_\parallel|}|\cos(|\mathbf{r}_\parallel\mathbf{G}_\parallel|)\ ,
\end{aligned}
\tag{C4}
$$

where $\mathbf{G}_\parallel$ refers to the reciprocal lattice vectors of the two-dimensional lattice, Ω is the volume of the two-dimensional Brillouin zone, σ is the Ewald parameter, and $V_\perp(r_\perp)$ is the $\mathbf{G}_\parallel=0$ component of the potential.

As was pointed out in Ref. 12, $V_\perp(r_\perp)$ can be calculated easily from a one-dimensional Poisson equation

$$
\frac{d^2V_\perp(r_\perp)}{dr_\perp^2}=-8\pi\rho_\perp(r_\perp)\ ,
\tag{C5}
$$

where $\rho_\perp(r_\perp)$ denotes the $\mathbf{G}_\parallel=0$ component of the charge distribution, which can be written as

$$\rho_\perp(r_\perp)=\sum_{p,\gamma}\frac{\bar{q}_{p\gamma}}{\Omega}\delta_{r_\perp,r_{p\gamma,\perp}}+\bar{\rho}(r_\perp)\ . \tag{C6}$$

In (C6) $\bar{\rho}(r_\perp)$ stands for the charge density distribution of the jellium, for which we assume a steplike behavior

$$\begin{aligned}\bar{\rho}(r_\perp)=&\bar{\rho}_0[1-\Theta(r_\perp-D_0)]\\&+\sum_{p=1}^{m}\bar{\rho}_p[\Theta(r_\perp-D_{p-1})-\Theta(r_\perp-D_p)]\\&+\bar{\rho}_{m+1}\Theta(r_\perp-D_{m+1})\ ,\end{aligned} \tag{C7}$$

where the positions of the steps D_p are most naturally chosen as

$$D_p=\frac{C_{p,\perp}+C_{p+1,\perp}}{2} \tag{C8}$$

and the step function is defined by

$$\Theta(x)=\begin{cases}0 & \text{if } x<0\\ 1 & \text{if } x>0\ .\end{cases}$$

In (C7) we assumed that for the layers to the left-hand side ($p\le 0$) and to the right-hand side ($p\ge m+1$) of the interface region, the interstitial charge density has constant values, $\bar{\rho}_0$ and $\bar{\rho}_{m+1}$, respectively. Quite clearly, for the case of a surface $\bar{\rho}_{m+1}=0$ has to be taken. It should be noted that (C7) is exact only when the boundaries between layers are planes. In general, when these boundaries are corrugated, $\bar{\rho}(\mathbf{r})$ necessarily has $\mathbf{G}_\parallel\neq 0$ components and in addition, its $\mathbf{G}_\parallel=0$ component cannot be exactly described by step functions like in (C7). Therefore, the present scheme can be regarded merely as a physically transparent approach to the solution of the 2D problem. Using (C6) and (C7) Eq. (C5) can be solved explicitly:

$$\begin{aligned}V_\perp(r_\perp)=&-\frac{4\pi}{\Omega}\sum_{p,\gamma}\frac{\bar{q}_{p\gamma}}{\Omega}|r_\perp-r_{p\gamma,\perp}|-4\pi\bar{\rho}_0[r_\perp^2-(r_\perp-D_0)^2\Theta(r_\perp-D_0)]\\&-4\pi\sum_{p=1}^{m}\bar{\rho}_p[(r_\perp-D_{p-1})^2\Theta(r_\perp-D_{p-1})-(r_\perp-D_p)^2\Theta(r_\perp-D_p)]\\&-4\pi\bar{\rho}_{m+1}(r_\perp-D_{m+1})^2\Theta(r_\perp-D_{m+1})+\mathcal{A}r_\perp+\mathcal{B}\ ,\end{aligned} \tag{C9}$$

where the two integration constants $\mathcal{A}$ and $\mathcal{B}$ have to be determined from the boundary conditions on the left- and right-hand side of the interface.[12] On the left (bulk) boundary this implies

$$V_\perp(r_{0\gamma_0,\perp})=V_\perp^0(a_{\gamma_0,\perp})\ , \tag{C10}$$

where the position $r_{0\gamma_0,\perp}$ is the closest lattice point in the left-hand side medium to the interface region and, according to Ref. 12,

$$V_\perp^0(a_{\gamma_0,\perp})=\frac{2\pi}{\Omega}\sum_\beta\bar{q}_{0\beta}\left[\frac{2}{d}(a_{\gamma_0,\perp}-a_{\beta,\perp})^2-2|a_{\gamma_0,\perp}-a_{\beta,\perp}|+\frac{d}{3}\right], \tag{C11}$$

with d being the layer spacing.

On the right-hand side we have to distinguish between an interface and a surface case: for an interface we have a boundary condition analogous to (C10), while for the surface case the potential on the vacuum side has to tend asymptotically to a constant value $V_{\rm vac}$. Therefore, for the ideal semi-infinite vacuum we require

$$V_\perp(r_{p\gamma,\perp})=V_{\rm vac}=\text{const}\quad \text{for } p\ge m+1\ . \tag{C12}$$

Quite obviously, (C12) ensures charge neutrality for the whole system. Since there is no charge in the ideal vacuum, $V_{\rm vac}$ is the only term which contributes to $V^E(\mathbf{r})$ (C1) in this region.

Following Slater and De Cicco,[30] the spherical part of the potential inside the spheres can be approximated fairly well by

$$V_{p\gamma}(r)=\frac{2\bar{q}_{p\gamma}}{r}-4\pi\bar{\rho}_p r^2+V_{p\gamma}^{\rm Mad}\ , \tag{C13}$$

where the so-called Madelung potentials can be calculated as

$$V_{p\gamma}^{\rm Mad}=\lim_{r\to 0}\left[V^E(\mathbf{r}-\mathbf{r}_{p\gamma})-\frac{2\bar{q}_{p\gamma}}{|\mathbf{r}-\mathbf{r}_{p\gamma}|}\right]. \tag{C14}$$

Including also the dipole field one gets

$$V_{p\gamma}^{\rm Mad}=\sum_{q,\beta}(\bar{q}_{q\beta}M_{p\gamma,q\beta}^{00}+\bar{d}_{q\beta}M_{p\gamma,q\beta}^{10})+V_{p\gamma}[\bar{\rho}]\ , \tag{C15}$$

where the component of the dipole moment perpendicular to the surface is defined as $\bar{d}_{q\beta}=\sqrt{3}Q_{q\beta}^{10}$. For a surface the monopole and dipole Madelung constants are given by

$$M_{p\gamma,q\delta}^{00}=(1-\delta_{r_{p\gamma,\perp}r_{q\delta,\perp}})\varphi(\mathbf{r}_{p\gamma,\parallel}-\mathbf{r}_{q\delta,\parallel};r_{p\gamma,\perp}-r_{q\delta,\perp})+\delta_{r_{p\gamma,\perp}r_{q\delta,\perp}}\varphi_0(\mathbf{r}_{p\gamma,\parallel}-\mathbf{r}_{q\delta,\parallel})-\frac{4\pi}{\Omega}\sum_{q'=1}^{m}\delta_{qq'}(|r_{p\gamma,\perp}-r_{q'\delta,\perp}|-r_{p\gamma,\perp}-r_{q'\delta,\perp})\ , \tag{C16}$$

$$M^{10}_{p\gamma,q\delta}=\frac{\partial M^{00}_{p\gamma,q\beta}}{\partial r_{q\beta,\perp}}=(1-\delta_{r_{p\gamma,\perp},r_{q\delta,\perp}})\psi(\mathbf{r}_{p\gamma,\parallel}-\mathbf{r}_{q\delta,\parallel};r_{p\gamma,\perp}-r_{q\delta,\perp})+\frac{4\pi}{\Omega}\sum_{q'=1}^{m}\delta_{qq'}[1+(1-\delta_{r_{p\gamma,\perp},r_{q'\delta,\perp}})\mathrm{sgn}(r_{p\gamma,\perp}-r_{q'\delta,\perp})]\ , \tag{C17}$$

where, without loss of generality, $r_{0\gamma_0,\perp}=0$ was supposed and the dipole electrostatic field $\psi(\mathbf{r}_\parallel;r_\perp)$ was derived in Ref. 5:

$$\psi(\mathbf{r}_\parallel;r_\perp)=\frac{4\pi}{\Omega}\mathrm{sgn}(r_\perp)\sum_{\mathbf{G}_\parallel\neq 0}\exp(-|r_\perp||\mathbf{G}_\parallel|)\cos(|r_\parallel\mathbf{G}_\parallel|)\ . \tag{C18}$$

It should be noted that according to (C14) for the case of $\mathbf{r}_{p\gamma,\parallel}=\mathbf{r}_{q\delta,\parallel}$, the divergent term $2/\mathbf{r}_\parallel$ has to be subtracted from $\varphi_0(\mathbf{r}_\parallel)$. The contribution to the Madelung potential attributed to the steplike interstitial charge density (C7) is given by

$$V_{p\gamma}[\bar{\rho}]=V^0_\perp(a_{\gamma_0,\perp})+8\pi\sum_{q=p}^{m}\bar{\rho}_q(D_q-D_{q-1})r_{p\gamma,\perp}+4\pi\bar{\rho}_0D_0^2+4\pi\sum_{q=1}^{p-1}\bar{\rho}_q(D_q^2-D_{q-1}^2)-4\pi\bar{\rho}_p(r_{p\gamma,\perp}-D_{p-1})^2\ . \tag{C19}$$

Finally, for the vacuum potential level one obtains

$$V_{\mathrm{vac}}=V^0_\perp(a_{\gamma_0,\perp})+\frac{8\pi}{\Omega}\sum_{p=1}^{m}\sum_{\gamma}(\bar{q}_{p\gamma}r_{p\gamma,\perp}+\bar{d}_{p\gamma})+4\pi\bar{\rho}_0D_0^2+4\pi\sum_{p=1}^{m}\bar{\rho}_p(D_p^2-D_{p-1}^2)\ . \tag{C20}$$

It is worthwhile to mention that the above formulas can be applied without any further modification for calculations within the ASA, by simply taking the limit $\bar{\rho}_p=0$ for all p.

[1] W. R. L. Lambrecht and O. K. Andersen, Surf. Sci. **178**, 256 (1986).

[2] B. Wenzien, J. Kudrnovský, V. Drchal, and M. Šob, J. Phys. Condens. Matter **1**, 9893 (1989).

[3] J. Kudrnovský, P. Weinberger, and V. Drchal, Phys. Rev. B **44**, 6410 (1991).

[4] V. Drchal, J. Kudrnovský, L. Udvardi, P. Weinberger, and A. Pasturel, Phys. Rev. B **45**, 14 328 (1992).

[5] J. Kudrnovský, I. Turek, V. Drchal, P. Weinberger, S. K. Bose, and A. Pasturel, Phys. Rev. B **47**, 16 525 (1993).

[6] H. L. Skriver and N. M. Rosengaard, Phys. Rev. B **43**, 9538 (1991).

[7] H. L. Skriver and N. M. Rosengaard, Phys. Rev. B **45**, 9410 (1992).

[8] H. L. Skriver and N. M. Rosengaard, Phys. Rev. B **46**, 7157 (1992).

[9] O. K. Andersen and O. Jepsen, Phys. Rev. Lett. **53**, 2571 (1984).

[10] J. M. MacLaren, X.-G. Zhang, A. Gonis, and S. Crampin, Phys. Rev. B **40**, 9955 (1989).

[11] A. Gonis, X. G. Zhang, J. M. LacLaren, and S. Crampin, Phys. Rev. B **42**, 3798 (1990).

[12] J. M. MacLaren, S. Crampin, D. D. Vvedensky, and J. B. Pendry, Phys. Rev. B **40**, 12 164 (1989).

[13] J. M. MacLaren, S. Crampin, and D. D. Vvedensky, Phys. Rev. B **40**, 12 176 (1989).

[14] D. C. Chrzan, L. M. Falicov, J. M. MacLaren, X.-G. Zhang, and A. Gonis, Phys. Rev. B **43**, 9442 (1991).

[15] K. Hampel, D. D. Vvedensky, and S. Crampin, Phys. Rev. B **47**, 4810 (1993).

[16] J. M. MacLaren, A. Gonis, and G. Schadler, Phys. Rev. B **45**, 14 392 (1992).

[17] P. Weinberger, *Electron Scattering Theory for Ordered and Disordered Matter* (Clarendon, Oxford, 1990).

[18] O. K. Andersen, A. V. Postnikov, and S. Yu. Savrasov, in *Applications of Multiple Scattering Theory to Materials Science,* edited by W. H. Butler, P. H. Dederichs, A. Gonis, and R. L. Weaver, MRS Symposia Proceedings No. 253 (Materials Research Society, Pittsburgh, 1992).

[19] F. Garcia-Moliner and V. R. Velasco, Prog. Surf. Sci. **21**, 93 (1986).

[20] S. L. Cunningham, Phys. Rev. B **10**, 4988 (1974).

[21] D. G. Anderson, J. Assoc. Comput. Mach. **12**, 547 (1964).

[22] D. D. Johnson, Phys. Rev. B **38**, 12 807 (1988).

[23] S. Crampin, J. Phys. Condens. Matter **5**, 4647 (1993).

[24] See, e.g., G. Hörmandinger and P. Weinberger, J. Phys. Condens. Matter **4**, 2175 (1992).

[25] G. H. Schadler, Phys. Rev. B **45**, 11 314 (1992).

[26] J. Kollár and B. Újfalussy, J. Comput. Phys. (to be published).

[27] J. Kollár and B. Újfalussy, J. Phys. Condens. Matter **4**, 5391 (1992).

[28] S. Crampin, J. Phys. Condens. Matter **5**, L443 (1993).

[29] P. P. Ewald, Ann. Phys. **64**, 253 (1921).

[30] J. C. Slater and P. De Cicco, in *Quantum Theory of Molecules and Solids,* edited by J. C. Slater (McGraw-Hill, New York, 1967), Vol. III.